AL-TR-1992-0156

ARMSTRONG LABORATORY

CURRENTS INDUCED IN THE HUMAN BODY FOR EXPOSURE TO ULTRAWIDEBAND ELECTROMAGNETIC PULSES

Om P. Gandhi
Cynthia M. Furse

Department of Electrical Engineering
University of Utah
Salt Lake City, UT 84112

OCCUPATIONAL AND ENVIRONMENTAL HEALTH DIRECTORATE
RADIOFREQUENCY RADIATION DIVISION
2503 D Drive
Brooks Air Force Base, TX 78235-5102

May 1993

Final Technical Report for Period August 1992 – November 1992

Approved for public release; distribution is unlimited.

AIR FORCE MATERIEL COMMAND
BROOKS AIR FORCE BASE, TEXAS

NOTICES

This report has been reviewed and is approved for publication.

WILLIAM D. HURT, M.S.	DAVID N. ERWIN, Ph.D.
Project Scientist	Chief, Radiofrequency Radiation Division

REPORT DOCUMENTATION PAGE

Form Approved
OMB No. 0704-0188

1. AGENCY USE ONLY *(Leave blank)*	2. REPORT DATE	3. REPORT TYPE AND DATES COVERED
	May 1993	Final, August 1992-November 1992

4. TITLE AND SUBTITLE

Currents Induced in the Human Body for Exposure to Ultrawideband Electromagnetic Pulses

5. FUNDING NUMBERS

C - F33615-91-C-0600
PR - 7757
TA - 01
WU - 2C

6. AUTHOR(S)

Om P. Gandhi
Cynthia M. Furse

7. PERFORMING ORGANIZATION NAME(S) AND ADDRESS(ES)

Department of Electrical Engineering
University of Utah
Salt Lake City, UT 84112

8. PERFORMING ORGANIZATION REPORT NUMBER

9. SPONSORING/MONITORING AGENCY NAME(S) AND ADDRESS(ES)

Armstrong Laboratory (AFMC)
Occupational and Environmental Health Directorate
Radiofrequency Radiation Division
2503 D Drive
Brooks Air Force Base, TX 78235-5102

10. SPONSORING/MONITORING AGENCY REPORT NUMBER

AL-TR-1992-0156

11. SUPPLEMENTARY NOTES

Armstrong Laboratory Technical Monitor: William D. Hurt, (210) 536-3185.

12a. DISTRIBUTION/AVAILABILITY STATEMENT

Approved for public release; distribution is unlimited.

12b. DISTRIBUTION CODE

13. ABSTRACT *(Maximum 200 words)*

We have used the recently developed frequency-dependent finite-difference time-domain ($(FD)^2TD$) method to calculate internal electric fields and induced current densities in a 1.31-cm resolution anatomically based model of the human body for exposure to an ultrawideband vertically polarized electromagnetic pulse (EMP). The Fourier spectrum of the pulse revealed that it had energy content to about 1500 MHz with the bulk of the energy being in the frequency band 400-800 MHz. The complex permittivities $\epsilon^*(w)$ for the various tissues are known to vary a great deal over the wide bandwidth of the incident pulse. In the ($(FD)^2TD$) formulation, these frequency-dependent $\epsilon^*(w)$ have been described by the best-fit two-relaxation Debye equations with different constants ϵ_∞, ϵ_{s1}, and ϵ_{s2} for the sixteen tissues (fat, muscle, blood, etc.) that are used in defining the anatomically based model. From the values of the induced electric displacement vector D, we have calculated the time variations of the vertical currents that pass through each of the sections of the model that is assumed to be either isolated or shoe-wearing, standing above a perfectly conducting ground plane. Peak vertical currents with magnitudes on the order of 1-4 mA per V/m of incident electric fields are calculated with the highest values calculated for the sections through the bladder and slightly above it.

14. SUBJECT TERMS

Ultrawideband pulse exposure; Anatomically based model; Dispersive properties of various tissues; Induced fields and currents.

15. NUMBER OF PAGES

36

16. PRICE CODE

17. SECURITY CLASSIFICATION OF REPORT	18. SECURITY CLASSIFICATION OF THIS PAGE	19. SECURITY CLASSIFICATION OF ABSTRACT	20. LIMITATION OF ABSTRACT
Unclassified	Unclassified	Unclassified	UL

NSN 7540-01-280-5500

Standard Form 298 (Rev. 2-89)
Prescribed by ANSI Std. Z39-18
298-102

CURRENTS INDUCED IN THE HUMAN BODY FOR EXPOSURE TO ULTRAWIDEBAND ELECTROMAGNETIC PULSES

I. INTRODUCTION

We have previously used a sixteen tissue anatomically based model of the human body to calculate induced currents for exposure to vertically polarized electromagnetic pulses (EMP) [1]. Since the bandwidths associated with these EMPs with risetimes on the order of 10-30 ns and durations on the order of 100-300 ns were fairly small, typically 0-100 MHz, a conventional nondispersive finite-difference time-domain (FDTD) method could be used for the calculations. In this method the tissue properties are assumed to be independent of frequency and are taken at a center-based frequency of 40 MHz. While the conventional FDTD method which ignores the dispersion of the tissue's dielectric properties may be appropriate for narrowband irradiation, it is clearly not suitable for wideband irradiation such as that due to short pulses with subnanosecond risetimes and pulse durations on the order of a few nanoseconds. We have consequently modified the FDTD algorithm to incorporate the frequency dispersion of the dielectric properties for the various tissues [2,3]. We have used the new frequency-dependent finite-difference time-domain ($(FD)^2TD$) method to calculate the induced currents and specific absorptions (SA) for an ultrawideband pulse, the time history of which was prescribed on a diskette by Jim O'Loughlin of Kirtland AFB, New Mexico. This was arranged by Dr. David N. Erwin of Armstrong Laboratory, Brooks AFB, Texas.

II. THE FREQUENCY-DEPENDENT FINITE-DIFFERENCE TIME-DOMAIN ($(FD)^2TD$) METHOD

The time-dependent Maxwell's curl equations used for the FDTD method are:

$$\nabla \times \mathbf{E} = -\frac{\partial \mathbf{B}}{\partial t} = -\mu \frac{\partial \mathbf{H}}{\partial t} \quad (1)$$

$$\nabla \times \mathrm{H} = \frac{\partial \mathbf{D}}{\partial t} \quad (2)$$

where the displacement vector **D** is related to the electric field **E** through the complex permittivity $\varepsilon^*(\omega)$ of the local tissue by the following equation:

$$\mathbf{D} = \varepsilon^*(\omega)\,\mathbf{E} \tag{3}$$

For the conventional FDTD method the complex permittivity $\varepsilon^*(\omega)$ is assumed to be independent of the frequency ω, Equation 3 is substituted into Equation 2, and Equations 1 and 2 are then solved iteratively in the time domain.

For the new frequency-dependent FDTD method $\varepsilon^*(\omega)$ is dependent on the frequency ω, and Equation 3 must be converted to a form which can be solved iteratively in the time domain along with Equations 1 and 2. This conversion may be done by choosing a rational function for $\varepsilon^*(\omega)$ such as the Debye equation with two relaxation constants [2]:

$$\varepsilon^*(\omega) = \varepsilon_0\left[\varepsilon_\infty + \frac{\varepsilon_{s1} - \varepsilon_\infty}{1+j\omega\tau_1} + \frac{\varepsilon_{s2} - \varepsilon_\infty}{1+j\omega\tau_2}\right] \tag{4}$$

From Equation 3 we can write $\mathbf{D}(\omega)$

$$\mathbf{D}(\omega) = \varepsilon^*(\omega)\,\mathbf{E}(\omega) = \varepsilon_0 \frac{\varepsilon_s + j\omega\,(\varepsilon_{s1}\tau_2 + \varepsilon_{s2}\tau_1) - \omega^2\tau_1\tau_2\varepsilon_\infty}{1 + j\omega(\tau_1 + \tau_2) - \omega^2\tau_1\tau_2}\,\mathbf{E}(\omega) \tag{5}$$

where the zero (static) frequency dielectric constant ε_s is given by

$$\varepsilon_s = \varepsilon_{s1} + \varepsilon_{s2} - \varepsilon_\infty\,. \tag{6}$$

Since Equation 5 is a frequency-domain description of **D** obtained for a single-frequency sinusoidal variation of fields, we can write it for an arbitrary time variation in terms of the following differential equation:

$$\tau_1\tau_2\frac{\partial^2\mathbf{D}}{\partial t^2} + (\tau_1 + \tau_2)\frac{\partial\mathbf{D}}{\partial t} + \mathbf{D} = \varepsilon_0\left[\varepsilon_s\,\mathbf{E}(t) + [\varepsilon_s\,\tau_2 + \varepsilon_{s2}\,\tau_1]\frac{\partial\mathbf{E}}{\partial t} + \varepsilon_\infty\,\tau_1\,\tau_2\frac{\partial^2\mathbf{E}}{\partial t^2}\right] \tag{7}$$

As can be recognized, Equation 7 is a modified version of the polarization equation in the relaxation theory of dielectrics. For the $(FD)^2TD$ method, we need to solve Equations 1 and 2 subject to Equation 7. Similar to references 1-4 the space and time derivatives in these equations can be approximated by differences, and these equations may be solved for $\mathbf{E} \rightarrow \mathbf{H} \rightarrow \mathbf{D}$

iteratively. In the $(FD)^2TD$ method [2] we use the values of **E** to calculate **H** (Equation 1), use **H** to calculate **D** (Eq. 2) and use **D** to solve for **E** (Eq. 7). The detailed procedure and the difference equations for Equations 1, 2 and 7 are given in reference 2.

From the calculated internal fields we calculated the vertical currents passing through the various layers of the body by using the following equation:

$$I_z(t) = \delta^2 \sum_{i,j} \frac{\partial D_z}{\partial t} \tag{8}$$

where δ is the cell size (=1.31 cm), and the summation is carried out for all cells in a given layer. We also calculated the layer-averaged absorbed energy density or SA and the total energy W absorbed by the whole body using the following relationships:

$$SA\Big|_{\text{layer } k} = \frac{\delta t}{N_k} \sum_t \frac{\mathbf{E}(i,j,k,t)}{\rho(i,j,k)} \cdot \frac{\partial \mathbf{D}(i,j,k,t)}{\partial t} \tag{9}$$

$$W = \delta t\, \delta^3 \sum_t \mathbf{E}(i,j,k,t) \cdot \frac{\partial \mathbf{D}(i,j,k,t)}{\partial t} \tag{10}$$

In Equations 9 and 10 δt is the time step (= δ/2c = 0.02183 ns) used for the time-domain calculations, N_k is the number of cells in layer k of the body, and ρ(i,j,k) is the mass density in kg/m^3 for each of the cells in the corresponding layers.

For the various calculations we have used both the isolated model of the human body as well as the model standing vertically on a conducting ground plane. For the latter, the shoe-wearing condition is modelled by a separation layer of rubber ($\varepsilon_r = 4.0$) of thickness 2.62 cm (2δ) assumed between the feet and the ground plane.

III. MODELING OF BIOLOGICAL TISSUE PROPERTIES WITH THE DEBYE EQUATION

The measured properties of biological tissues (muscle, fat, bone, blood, intestine, cartilage, lung, kidney, pancreas, spleen, lung, heart, brain/nerve, skin, and eye) were obtained from reference 5. Optimum values for ε_{sl}, ε_{s2}, ε_o, τ_1, and τ_2 in Equation 4 were obtained by nonlinear least squares matching to the measured data for fat and muscle. All other tissues have properties falling roughly between these two. Optimum values shown in Table 1 for ε_{sl}, ε_{s2}, and ε_o for all tissues were then obtained with τ_1 and τ_2 being the average of optimized values for fat and muscle. This was done to facilitate volume averaging of the tissue properties in cells of the heterogeneous man model. Having τ_1 and τ_2 constant for all tissues allowed linear (volume) averaging of the ε values for each tissue in a given cell to calculate ε values for that cell. The measured tissue properties and those computed from the Debye equation with τ_1 and τ_2 being the average of fat and muscle are shown in Figure 1 for fat and muscle. Similar comparisons were also obtained for the other tissue types.

Table 1. Debye Constants for Tissues
$\tau_1 = 290.6 \times 10^{-9}/2\pi$
$\tau_2 = 0.5 \times 10^{-9}/2\pi$
(average of optimum for fat and muscle)

Tissue	ε_∞	ε_{s1}	ε_{s2}
Muscle	40.0	3948.	59.09
Bone/Cartilage	3.4	312.8	7.11
Blood	35.0	3563.	66.43
Intestine	39.0	4724.	66.09
Liver	36.3	2864.	57.12
Kidney	35.0	3332.	67.12
Pancreas/Spleen	10.0	3793.	73.91
1/3 Lung	10.0	1224.	13.06
Heart	38.5	4309.	54.58
Brain/Nerve	32.5	2064.	56.86
Skin	23.0	3399.	55.59
Eye	40.0	2191.	56.99

IV. THE ANATOMICALLY BASED MODEL

The procedure to obtain the anatomically based model of the human body is detailed in our earlier publication [1]. Briefly, we used anatomical sectional diagrams of the human body that were available in the book by Eycleshymer and Schoemaker [6]. For each of the available cross sections, the predominant tissue (1 of the 16 tissue types such as muscle, fat, bone, and blood, etc.) was identified for each of the square cells of dimensions 0.635 x 0.635 cm (1/4 in. x 1/4 in.) arranged in the form of a grid.

By interpolating between the anatomical cross sections that were available with variable separations of 2.3-2.7 cm (0.9 to 1.06 in), compositions of the various tissues were obtained for cubical subvolumes (cells) of dimensions 0.635 cm (1/4 in.) for each side. Since this arrangement resulted in a model with about 360,000 cells representing the whole body (about 3 million cells for the entire interaction space to the absorbing boundaries) this model was difficult to accommodate within the memory space of readily accessible computers. A 45,024-cell model with cubical cells of twice the initial dimension (1.27 cm or 0.5 in.) was developed next by averaging the data for 2 x 2 x 2 = 8 of the initial cells. Without changes in the relative properties of the various tissues, this process allows some flexibility in the height and weight of the model. We have taken a slightly larger cell size of 1.31 cm (0.516 in.) for the model to obtain a total height and body weight of 175.5 cm (169 in.) and 69.6 kg (153 lb), respectively.

V. RESULTS

A typical ultrawideband pulse with a peak amplitude of 1.1 V/m is shown in Figure 2. It is interesting to note that the pulse has a rise time of about 0.2 ns and a total time duration of about 7 - 8 ns. As aforementioned, this pulse was prescribed in digitized form on a computer diskette by Jim O'Loughlin of Kirtland AFB. We have calculated the Fourier spectrum of the prescribed pulse which is shown in Figure 3. Most of the energy in the pulse is concentrated in the 200 - 900 MHz band with the peak of the energy being at about 500 MHz. Since fairly similar Fourier spectra were calculated for all six of the pulses given on the diskette, we decided to treat the pulse waveform of Figure 2 as representative of all of the pulses.

We assumed the incident fields to be vertically polarized, since this polarization is known to result in the strongest coupling for standing individuals. Using the procedure of Section II (Equation 8), we have calculated the temporal variations of total vertical currents for the various sections of the body both for the shoe-wearing grounded, and ungrounded exposure conditions of the model, respectively. The current variations for some representative sections such as those through the eyes, neck, heart, liver, bladder, knees, and ankles are given in Figure 4a-g, respectively. The calculated peak currents are on the order of 1.1 to 3.2 mA/(V/m). It is interesting to note that there is very little difference in the induced currents whether the model is grounded or not, because most of the energy in the pulse is at frequencies in excess of 300 MHz where the effect of the ground plane on the induced currents or the SARs is minimal [7, 8].

In Figure 5 we have plotted the peak current for each section of the body with a resolution of 1.31 cm (0.516 in.) Also identified in this figure are the sections passing through the eyes, neck, etc., for which temporal variations are shown in Figure 4. As seen in Figure 5,the maximum peak current of 3.5 mA which is 3.2 mA/(V/m) occurs at a height of 96.3 cm (38 in.) above the bottom of the feet. A very similar result had previously been observed for calculations using isolated and grounded models of the human body for plane-wave exposures at frequencies of 350-700 MHz where the highest induced currents on the order of 3.0-3.2 mA/(V/m) were calculated for sections of the body that are at heights of 85-100 cm relative to the feet [7,8].

The Fourier spectra of the currents shown in Figure 4 for the various sections of the body are given in Figure 6. As expected, components from low frequencies to frequencies in excess of 1,000 MHz are observed. From Figure 6 it is obvious that any instrumentation to measure the induced currents through the feet or at any location of the body must have a bandwidth in excess of 1,000 MHz and subnanosecond response time.

Using Equations 9 and 10 we have also calculated the SA and the total absorbed energy for exposure to the ultrawideband pulse of Figure 2. The SAs are plotted in Figure 7 as a function of height above the feet of the various sections of the body for isolated and shoe-wearing conditions.

Note that because of the very limited time duration of the pulse (7-8 ns) the specific absorptions are on the order of 0.02 to 0.20 pJ/kg. Using Equation 10 the total energy absorbed by the body as a function of time has been calculated and is shown in Figure 8. The energy is virtually all absorbed in the first 6 to 8 ns. The total energy absorbed by the body exposed to a single pulse is calculated to be 2.0 and 1.91 pJ for isolated and shoe-wearing grounded conditions, respectively.

VI. PROJECTIONS FOR HIGHER PULSE AMPLITUDES AND REPETITION RATES

It is recognized that the SA and the energy absorbed by the body should be multiplied by square of the peak incident electric field amplitude and the pulse repetition rate in case the body is irradiated by more than one pulse at a time.

To illustrate, let us say that the pulse peak amplitude is 1 kV/m rather than 1.1 V/m that has been assumed for the above calculations. Furthermore, let us assume that the pulse repetition rate is 1,000 pulses per second rather than a single pulse. For such a train of pulses for any 6-min period there would be 3.6×10^5 pulses. Specific absorptions for the various sections of the body (from Figure 7) would be on the order of $(0.02 \text{ to } 1.8) \times 10^{-12} \times (10^3/1.1)^2 \times 3.6 \times 10^5 = (0.6 \text{ to } 5.4)$ mJ/kg. Similarly the total energy absorbed by the body in any 6-min period would be 0.59 and 0.57 J for isolated and shoe-wearing grounded conditions, respectively. Both the SAs and the whole-body absorption are considerably less than the 6-min averaged values of 144 J/kg and 10,080 J, respectively that are suggested in the ANSI/IEEE C95.1-1991 RF safety guidelines [9].

For a 1 kV/m peak amplitude pulse the induced peak currents for the various layers of the body can be scaled from the values given in Figure 5 for a 1.1 V/m peak amplitude pulse. Induced peak currents on the order of 1.1 - 3.2 A are calculated for 1 kV/m peak amplitude pulse and the values would be proportionately higher for larger amplitudes of the pulse.

REFERENCES

1. J-Y. Chen and O. P. Gandhi, "Currents Induced in an Anatomically Based Model of a Human for Exposure to Vertically Polarized Electromagnetic Pulses," *IEEE Transactions on Microwave Theory and Techniques*, Vol. 39, pp. 31-39, 1991.

2. O. P. Gandhi, B-Q. Gao and J-Y. Chen, "A Frequency Dependent Finite Difference Time Domain Formulation for General Dispersive Media," *IEEE Transactions on Microwave Theory and Techniques*, Vol. 41(4), 1993.

3. C. M. Furse, J-Y. Chen and O. P. Gandhi, " A Frequency Dependent Finite Difference Time-Domain Method for Induced Current and SAR Calculations for a Heterogeneous Model of the Human Body," submitted to *IEEE Transactions on Electromagnetic Compatibility*.

4. A. Taflove and K. R. Umashankar, "The Finite-Difference Time-Domain Method for Numerical Modeling of Electromagnetic Wave Interactions with Arbitrary Structures," Finite-Element Methods in Electromagnetic Scattering, M. A. Morgan, editor, Elsevier, New York Chapter 8, pp. 287-373, 1990.

5. C. H. Durney, et al., Radiofrequency Radiation Dosimetry Handbook (Second Edition), Report SAM-TR-78-22, USAF School of Aerospace Medicine, Brooks AFB, Texas 78235.

6. A. Eycleshymer and D. M. Schoemaker, "A Cross-Section Anatomy," D. Appleton Company, New York, 1970.

7. O. P. Gandhi, Y-G. Gu, J-Y. Chen, and H. I. Bassen, "Specific Absorption Rate and Induced Current Distributions in an Anatomically Based Human Model for Plane-Wave Exposures," *Health Physics*, Vol. 63 (3), pp. 281-290,1992.

8. O. P. Gandhi, Y-G. Gu and J-Y. Chen, "SAR and Induced Current Distributions in Anatomically Based Models of a Human for Plane-Wave Exposures at Frequencies 20-915 MHz," Final report on contract DAMD 17-90--M-SA 49, submitted to Department of Microwave Research, Walter Reed Army Institute of Research, Washington, D.C. 20307, August 27, 1990.

9. ANSI/IEEE C95.1-1991, "IEEE Standard for Safety Levels with Respect to Human Exposure to Radiofrequency Electromagnetic Fields, 3kHz to 300 GHz," Institute of Electrical and Electronics Engineers, 345 East 47th Street, New York, NY 10017, April 1992.

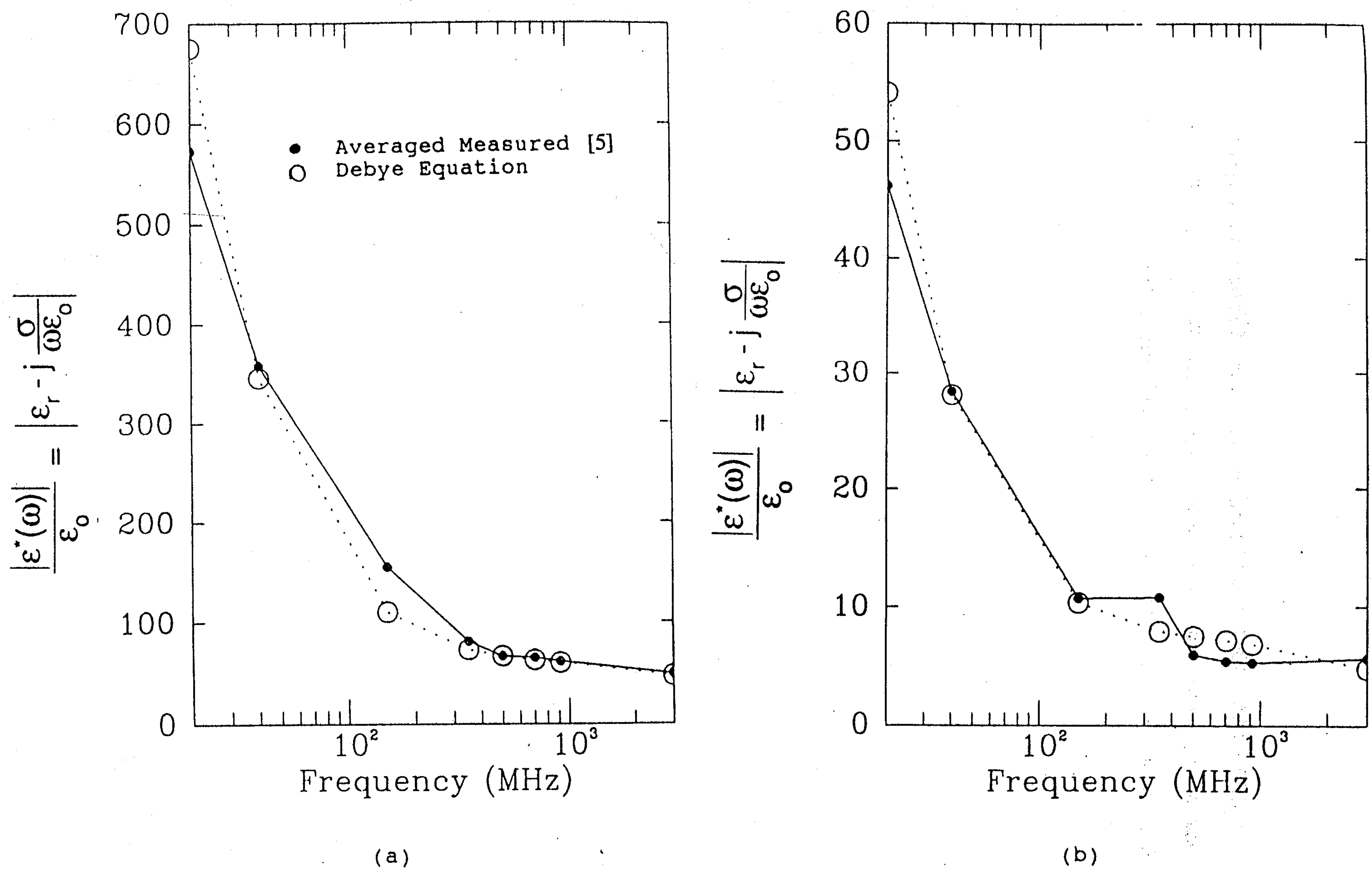

Figure 1. Fit of Debye equations with two relaxation constants (4) to measured tissue properties of (a) muscle and (b) fat.

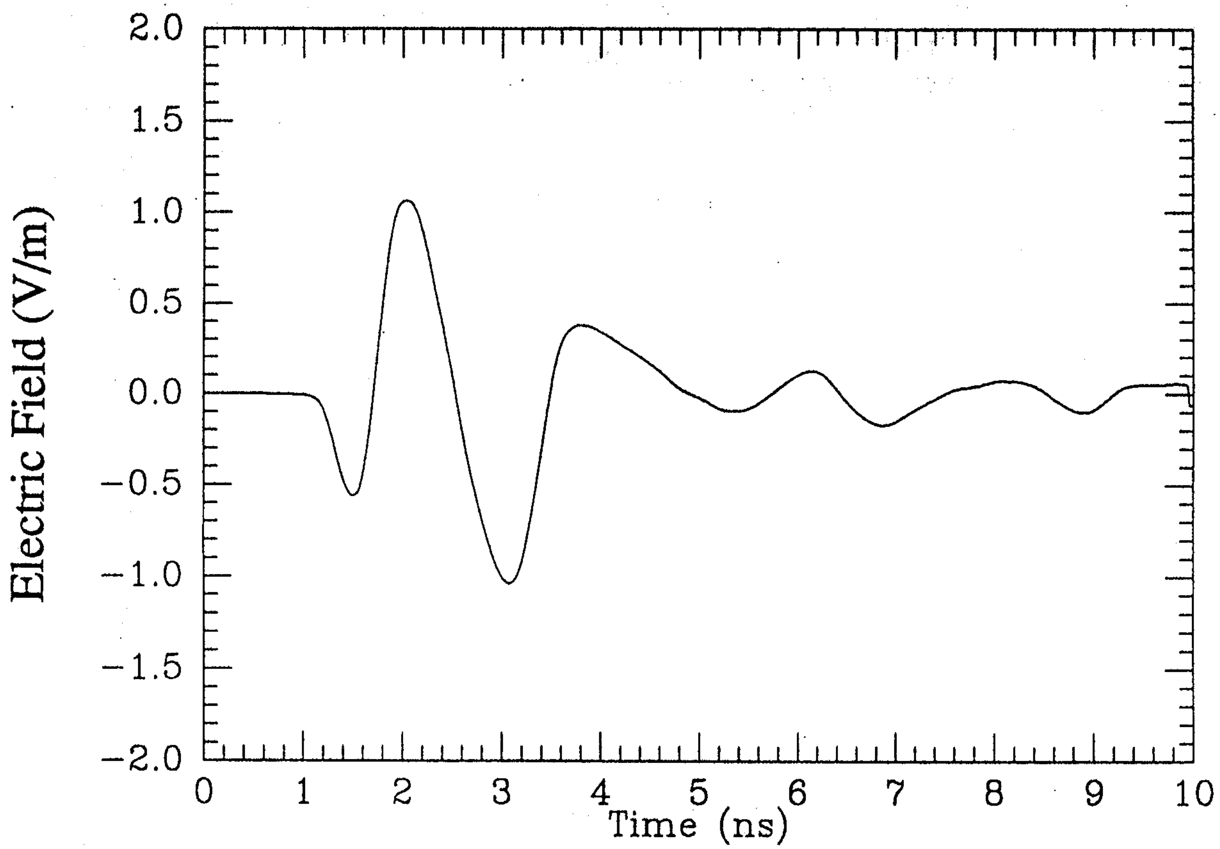

Figure 2. The prescribed electromagnetic pulse. Peak incident field = 1.1 V/m.

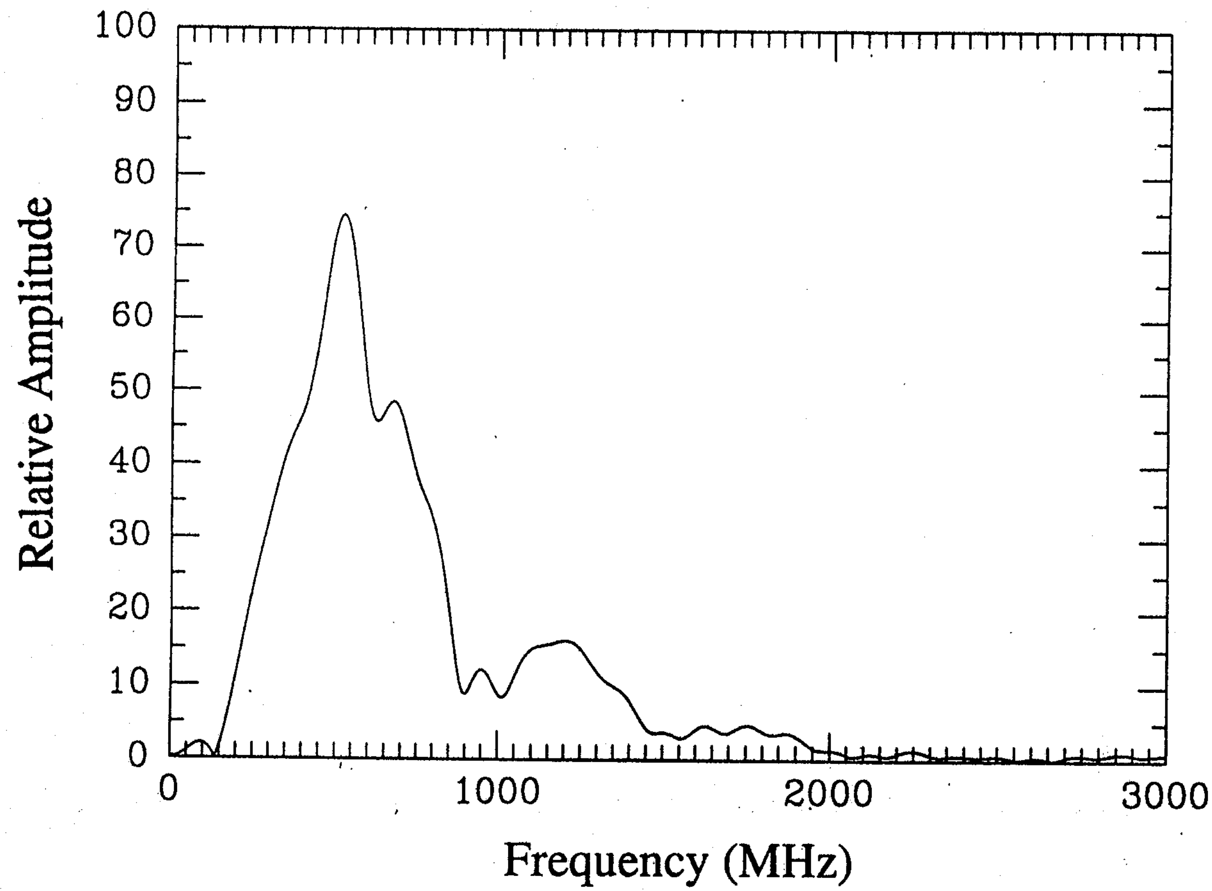

Figure 3. Fourier spectrum of the electromagnetic pulse of Figure 2.

4a. Section through the eyes (height above the bottom of the feet = 168.3 cm).

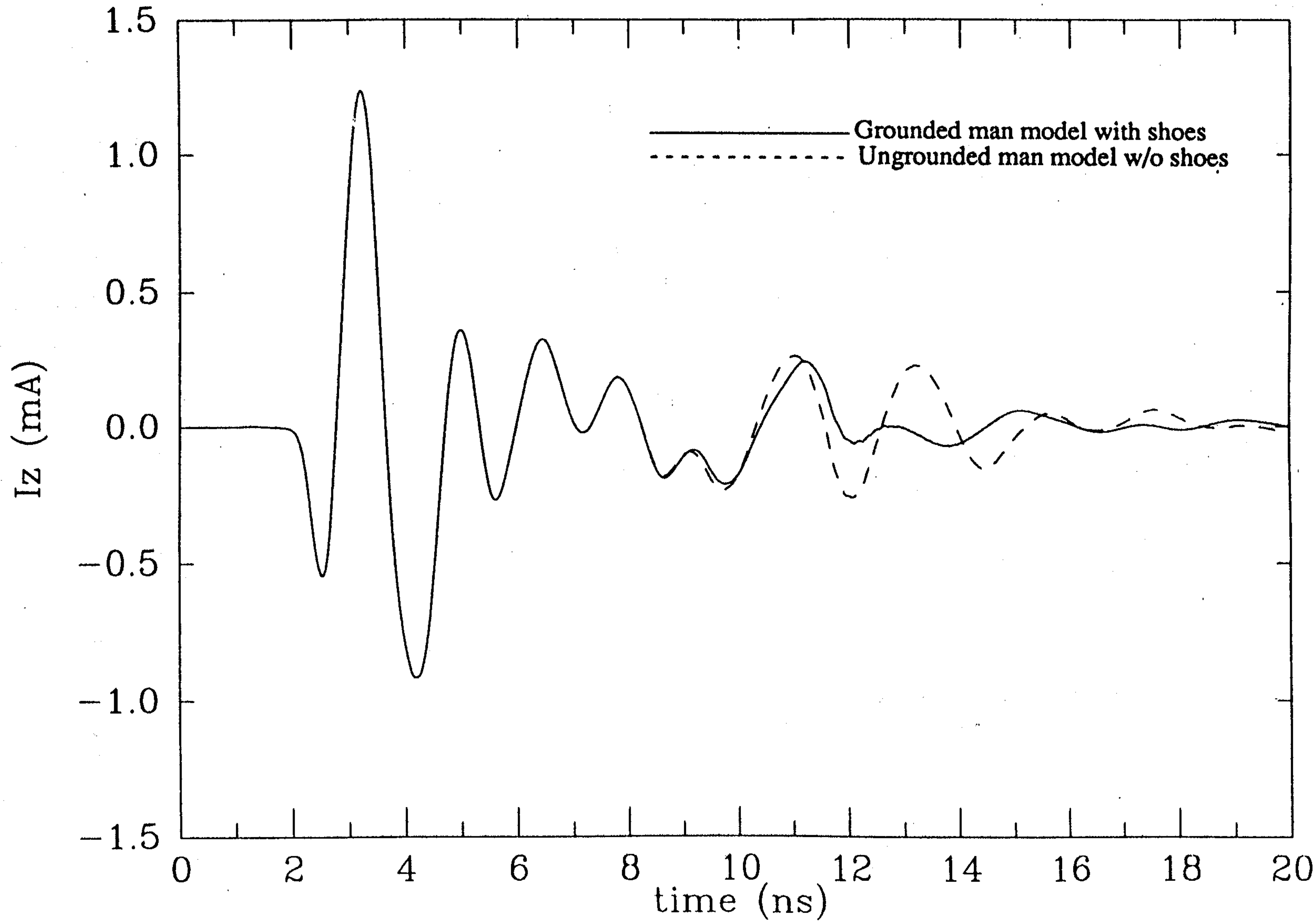

Figure 4. Currents induced for the various sections of the body for shoe-wearing grounded conditions of exposure. $E_{peak} = 1.1$ V/m.

4b. Section through the neck (height above the bottom of the feet = 155.2 cm).

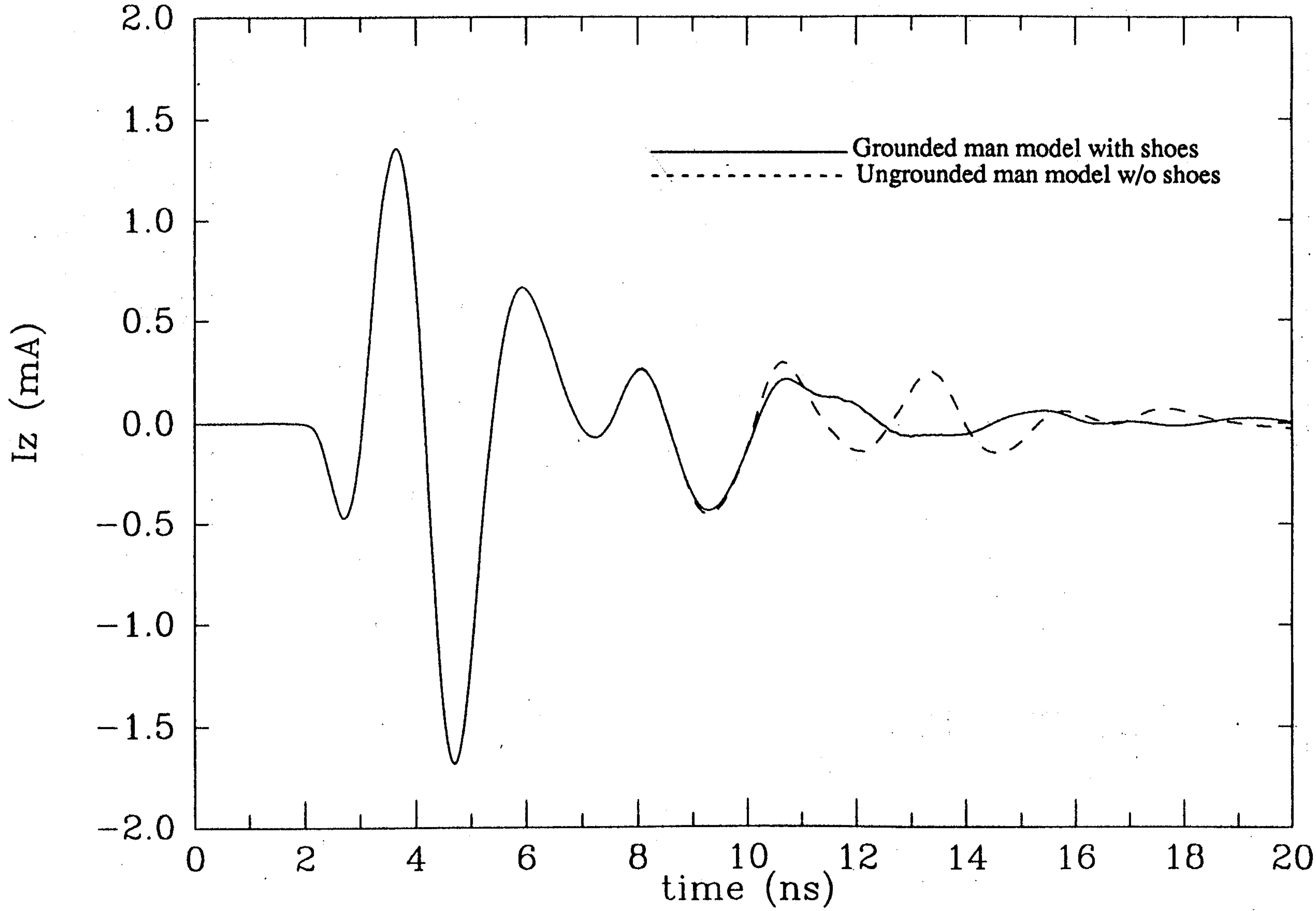

4c. Section through the heart (height above the bottom of the feet = 135.6 cm).

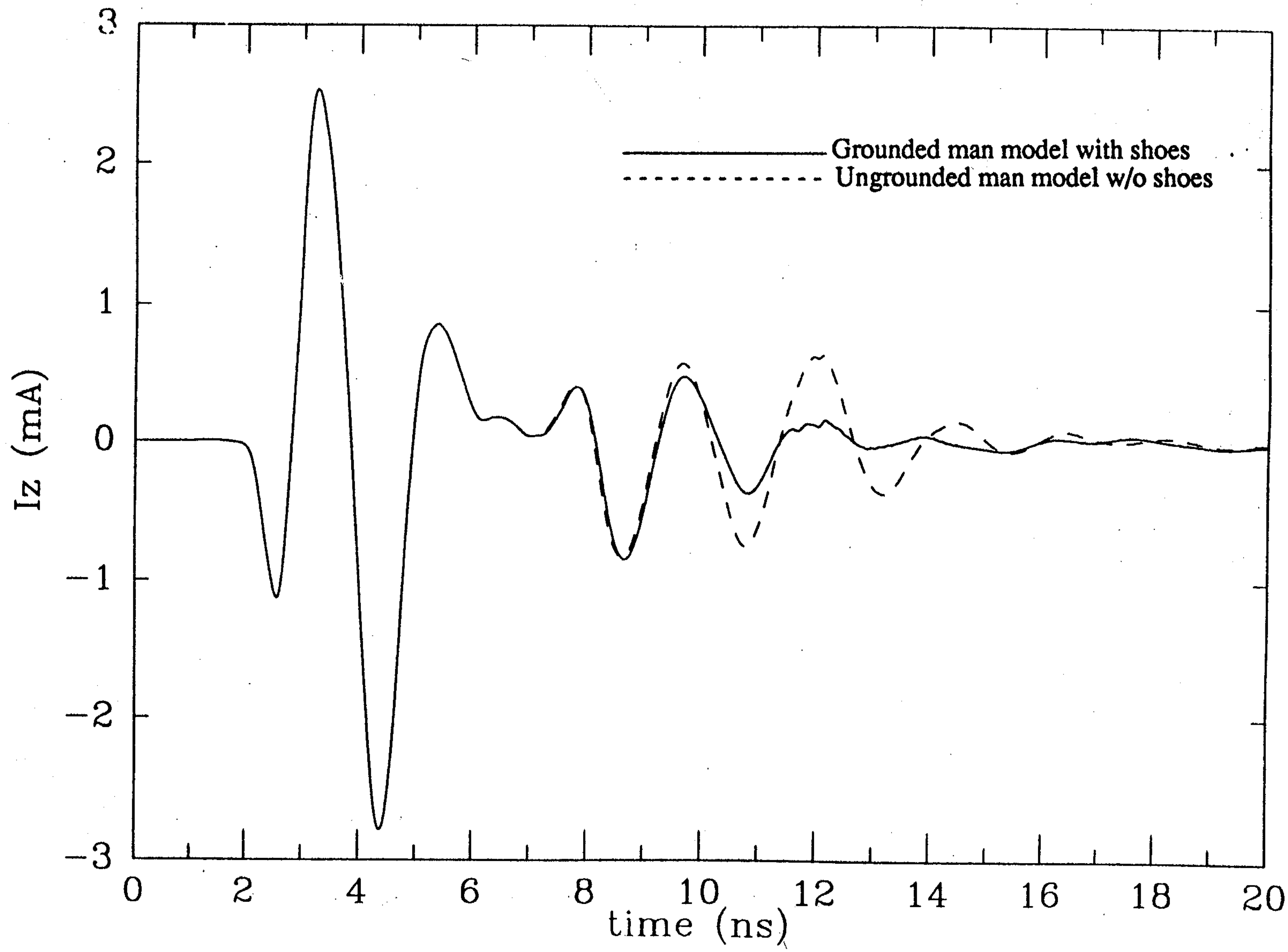

4d. Section through the liver (height above the bottom of the feet = 123.8 cm).

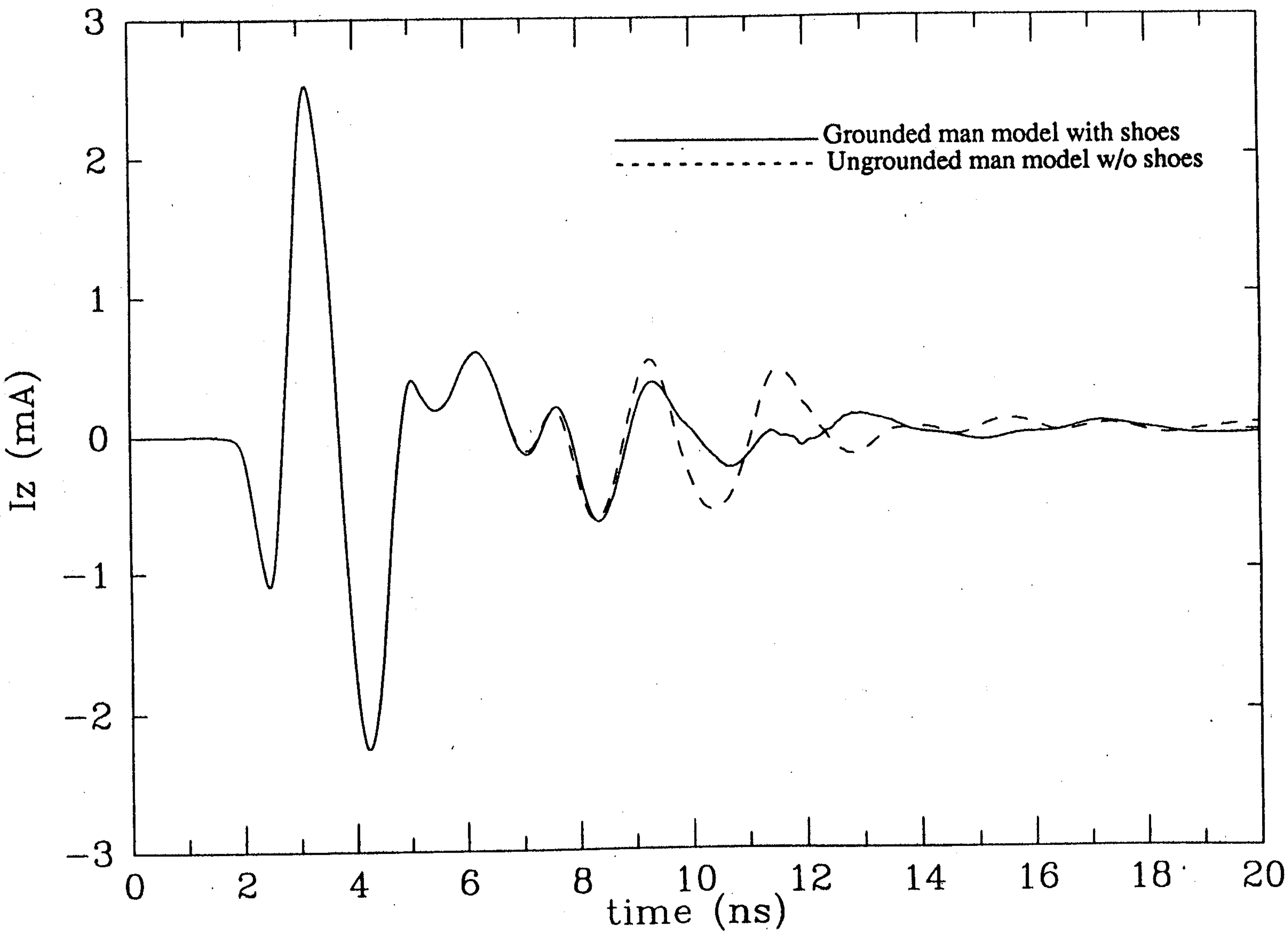

4e. Section through the bladder (height above the bottom of the feet = 91.0 cm).

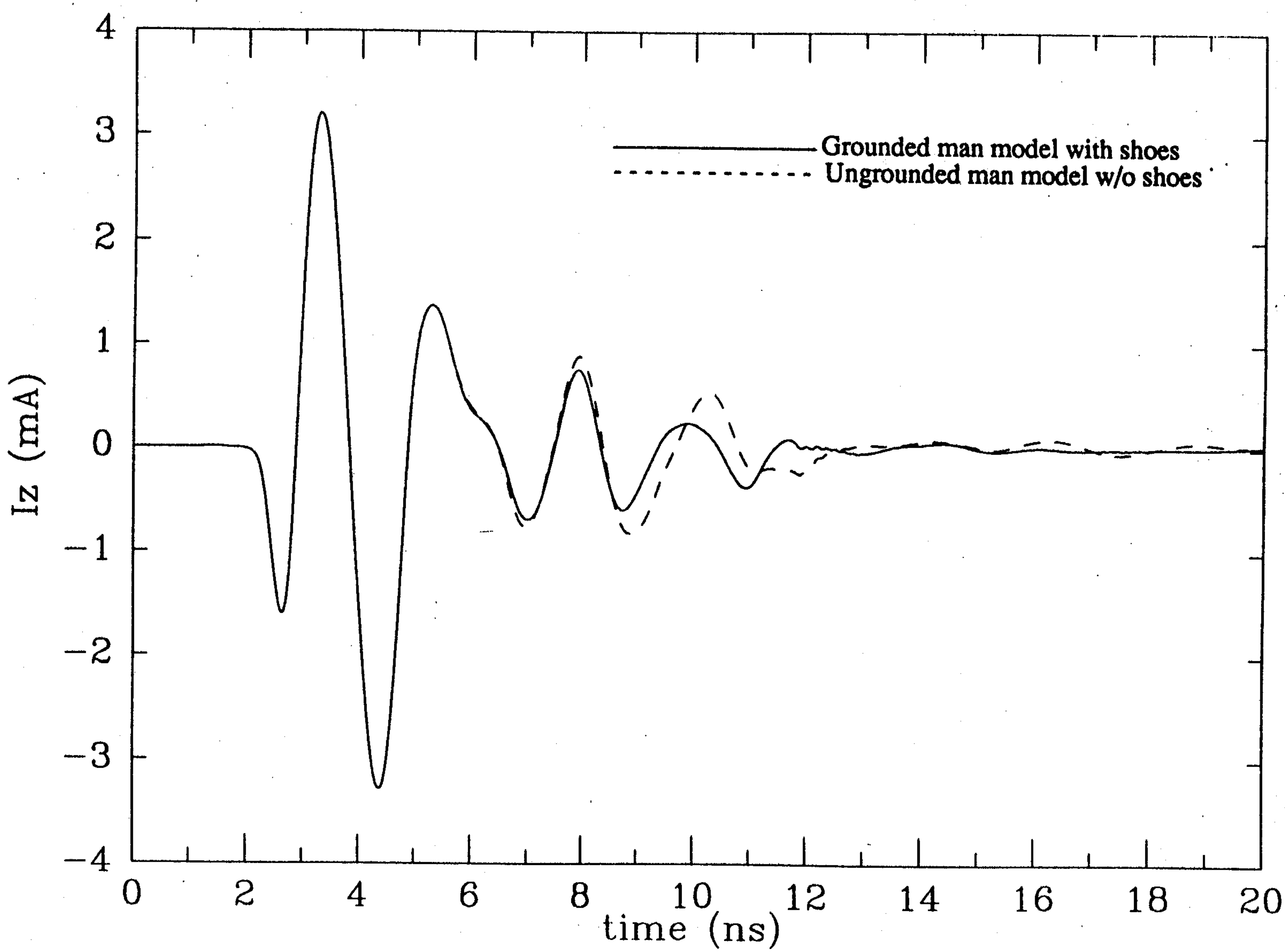

4f. Section through the knees (height above the bottom of the feet = 50.4 cm).

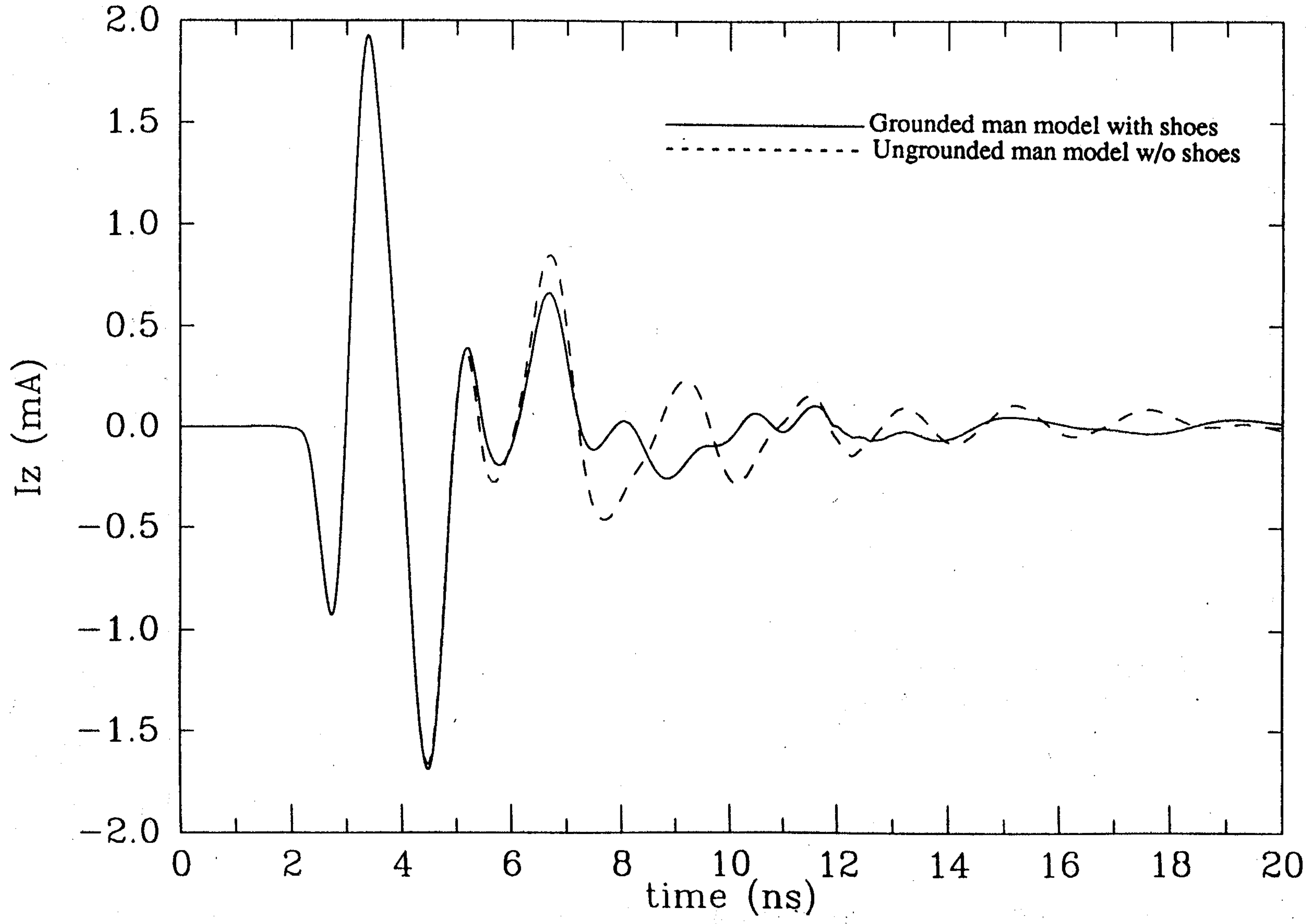

4g. Section through the ankles (height above the bottom of the feet = 13.76 cm).

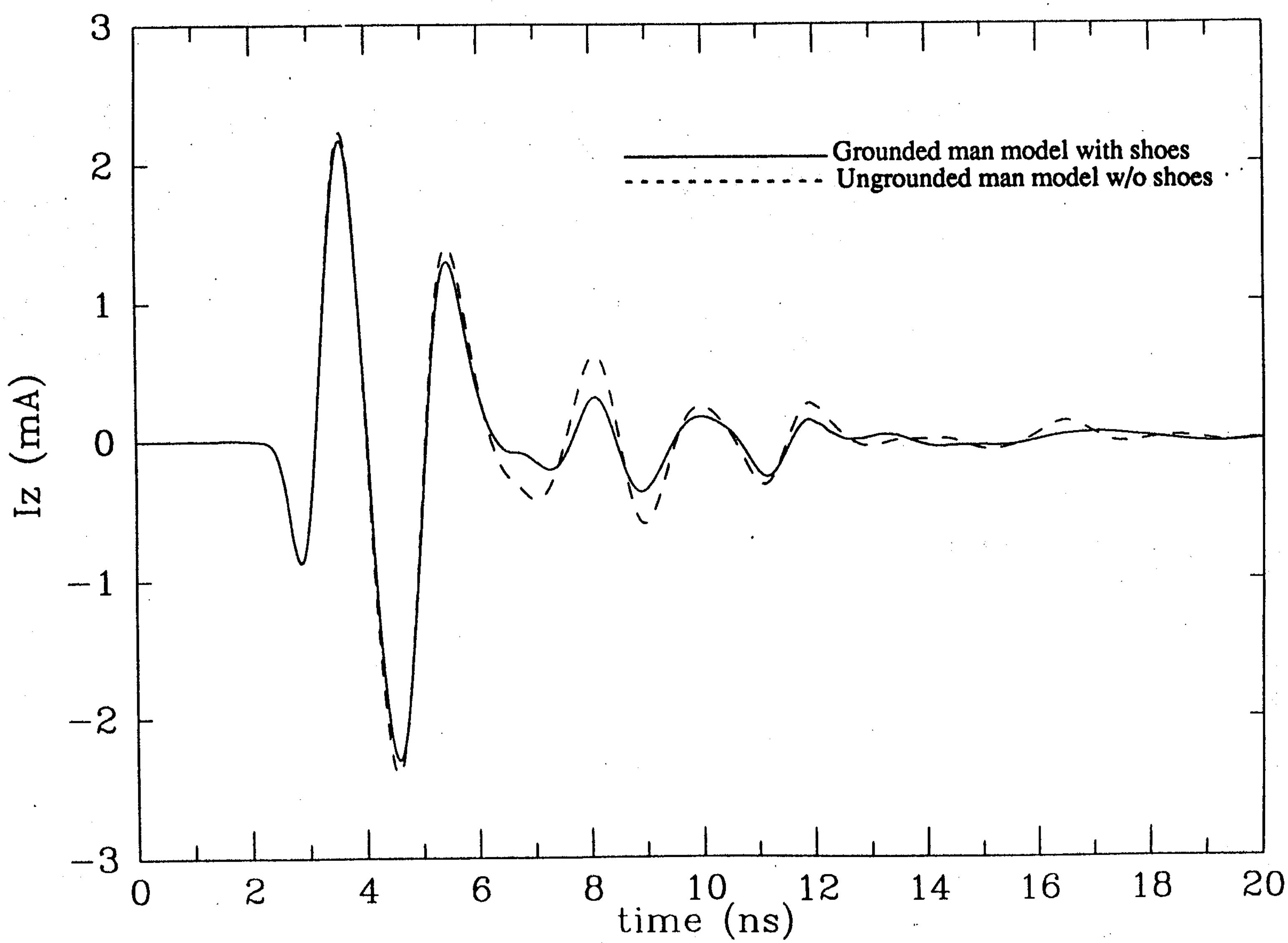

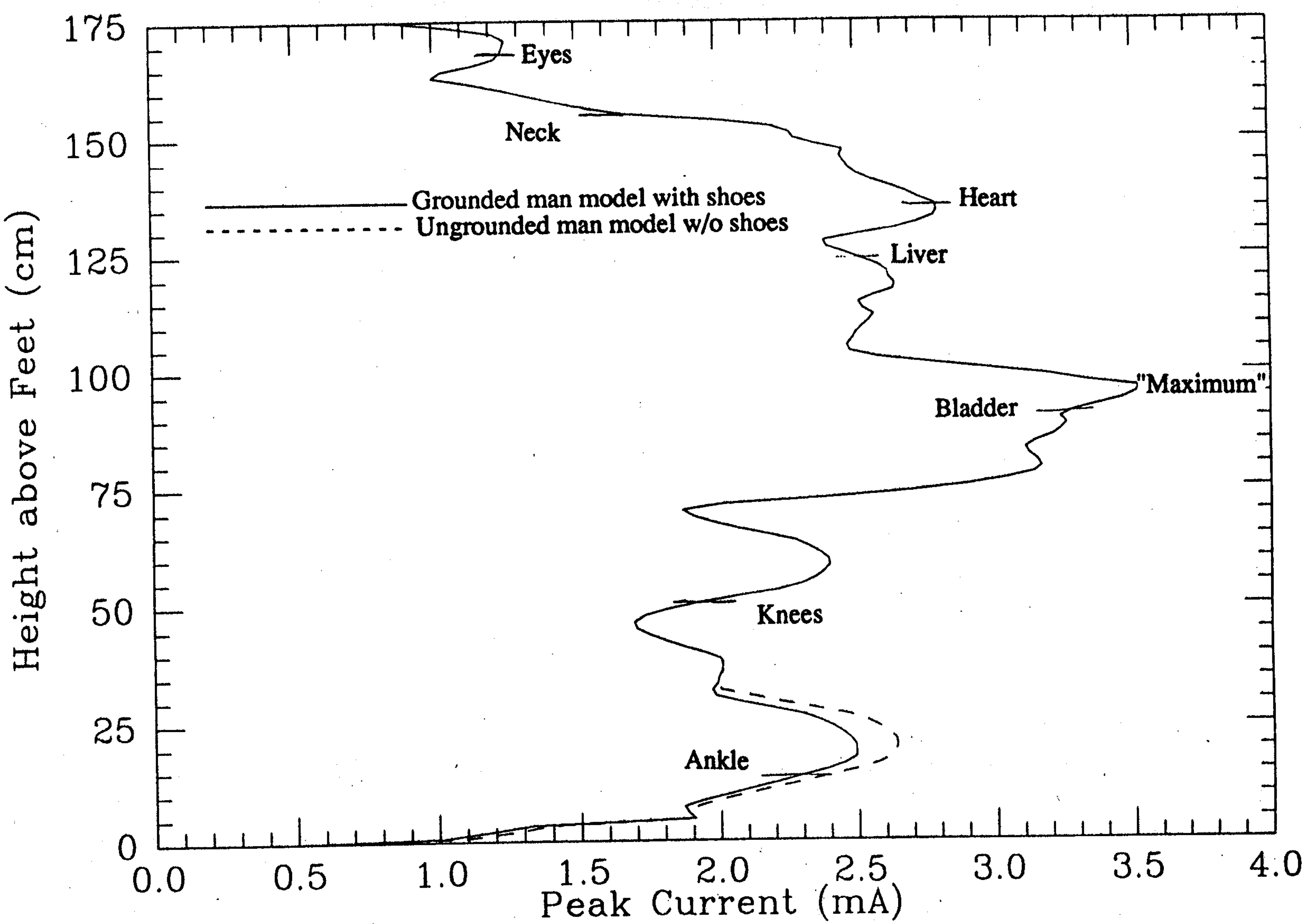

Figure 5. Peak currents induced for the various sections of the body for shoe-wearing grounded and ungrounded conditions of the model. $E_{peak} = 1.1$ V/m.

6a. Section through the eyes (height above the bottom of the feet = 168.3 cm).

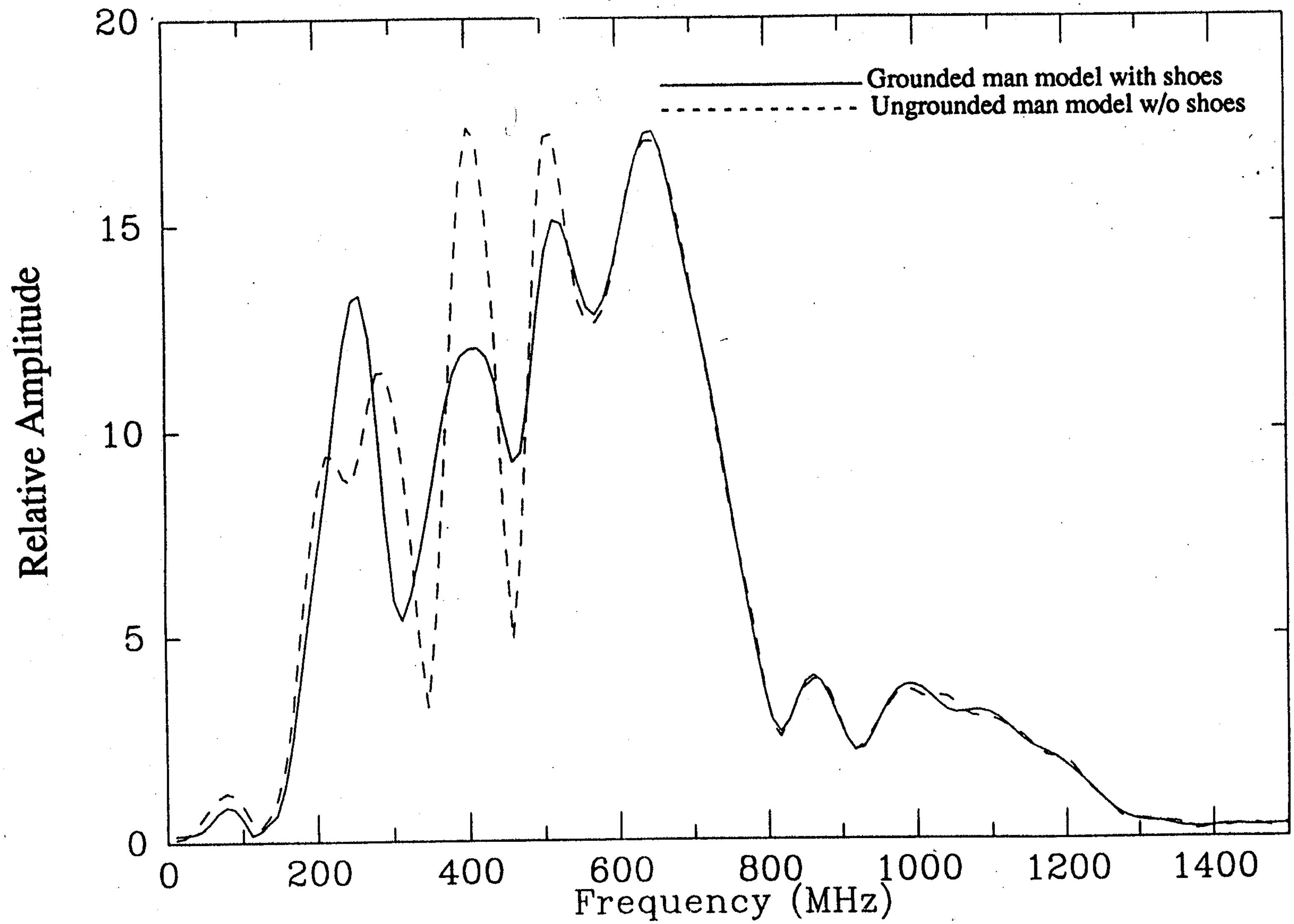

Figure 6. Fourier spectra of the currents induced for some representative sections of the body for shoe-wearing grounded and ungrounded conditions of exposure.

6b. Section through the neck (height above the bottom of the feet = 155.2 cm).

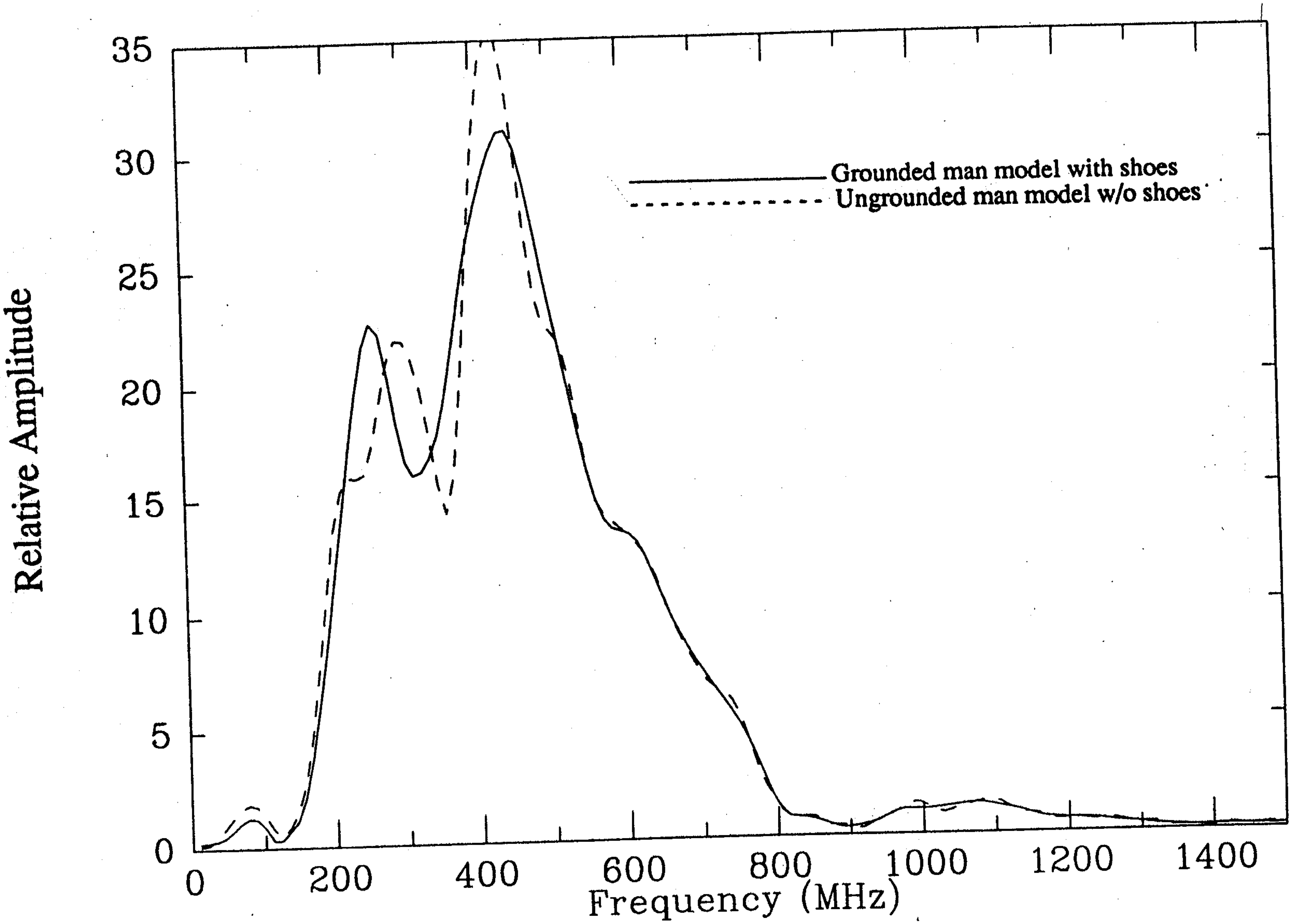

6c. Section through the heart (height above the bottom of the feet = 135.6 cm).

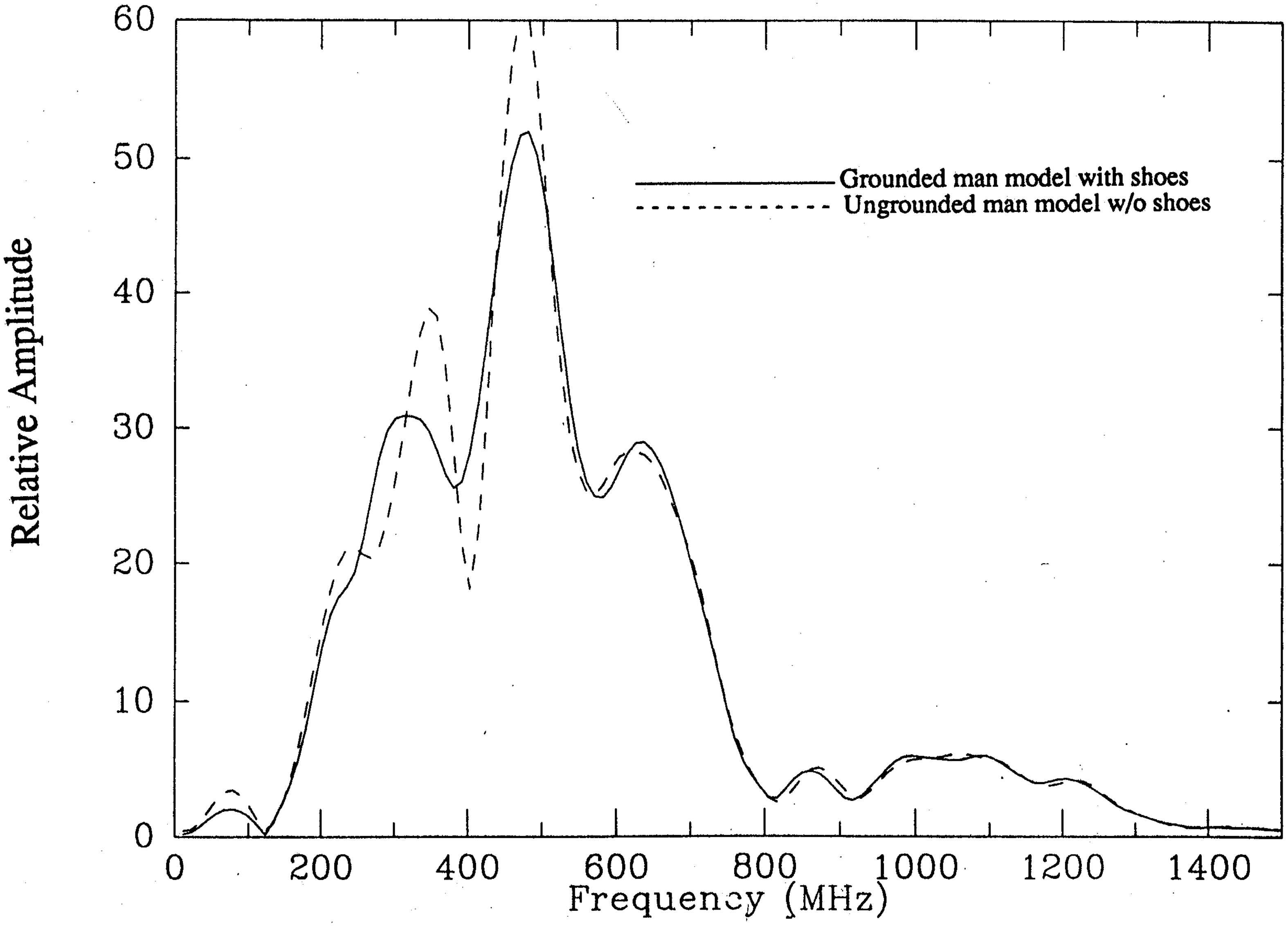

6d. Section through the liver (height above the bottom of the feet = 123.8 cm).

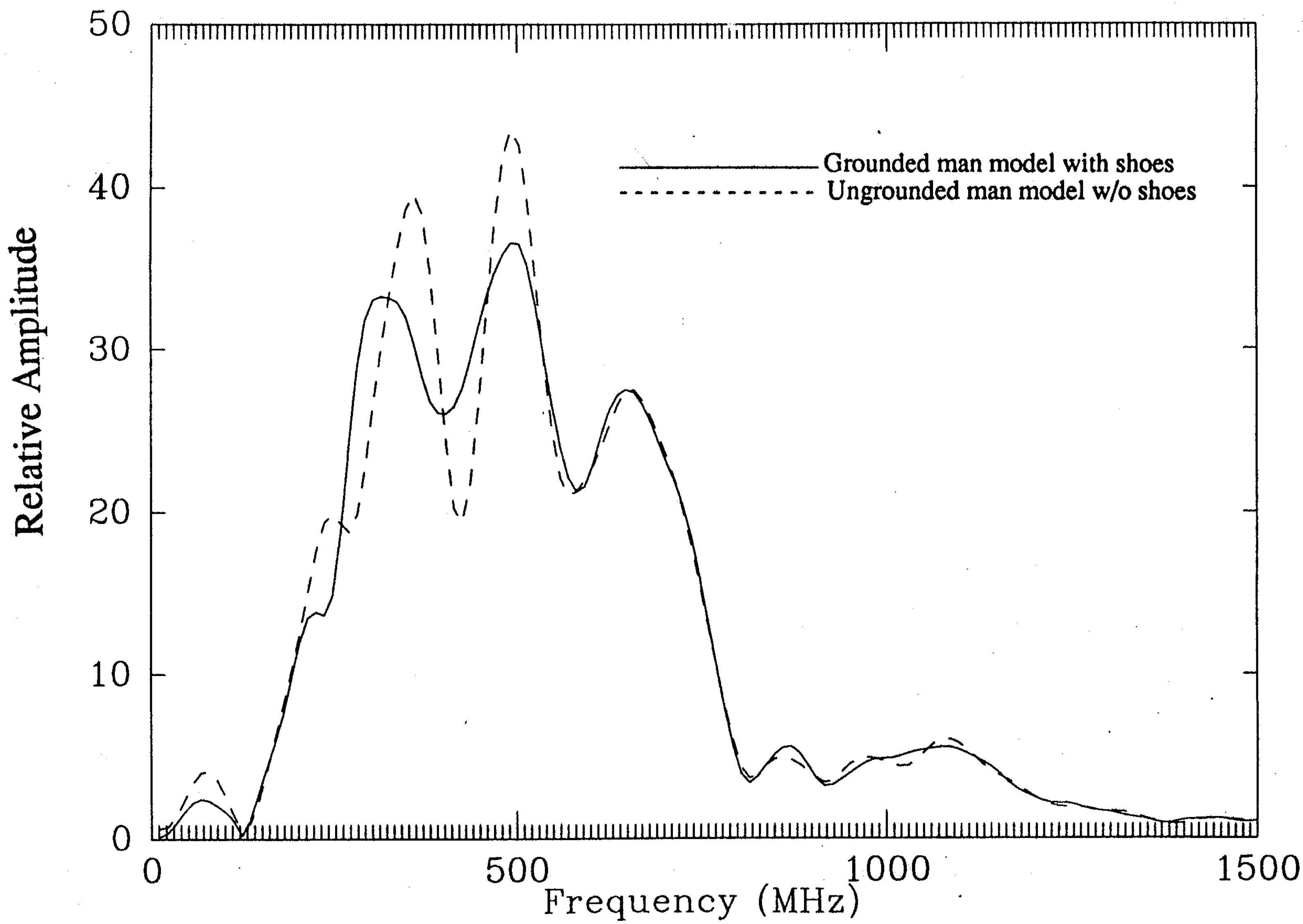

6e. Section through the bladder (height above the bottom of the feet = 91.0 cm).

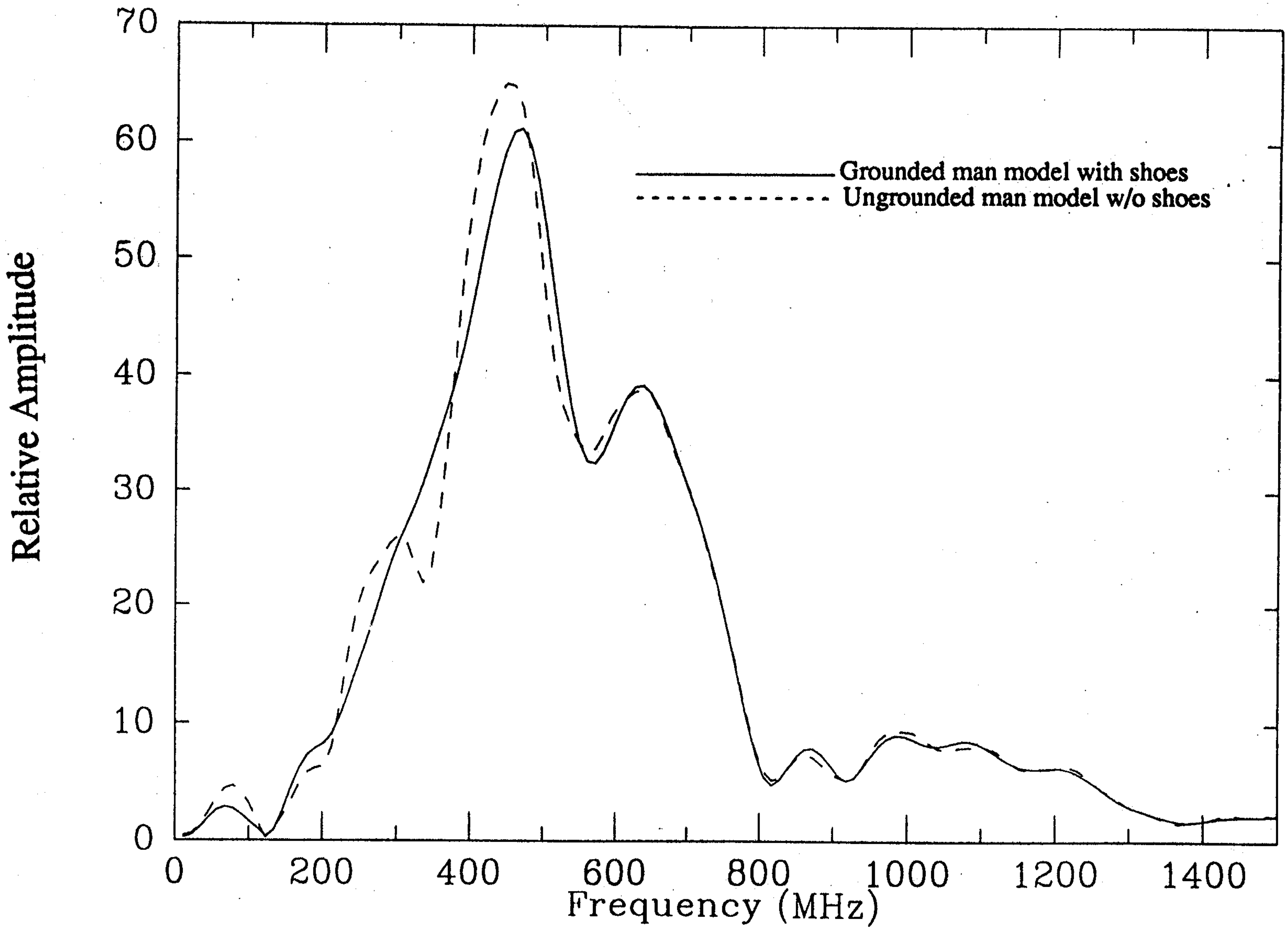

6f. Section through the knees (height above the bottom of the feet = 50.4 cm).

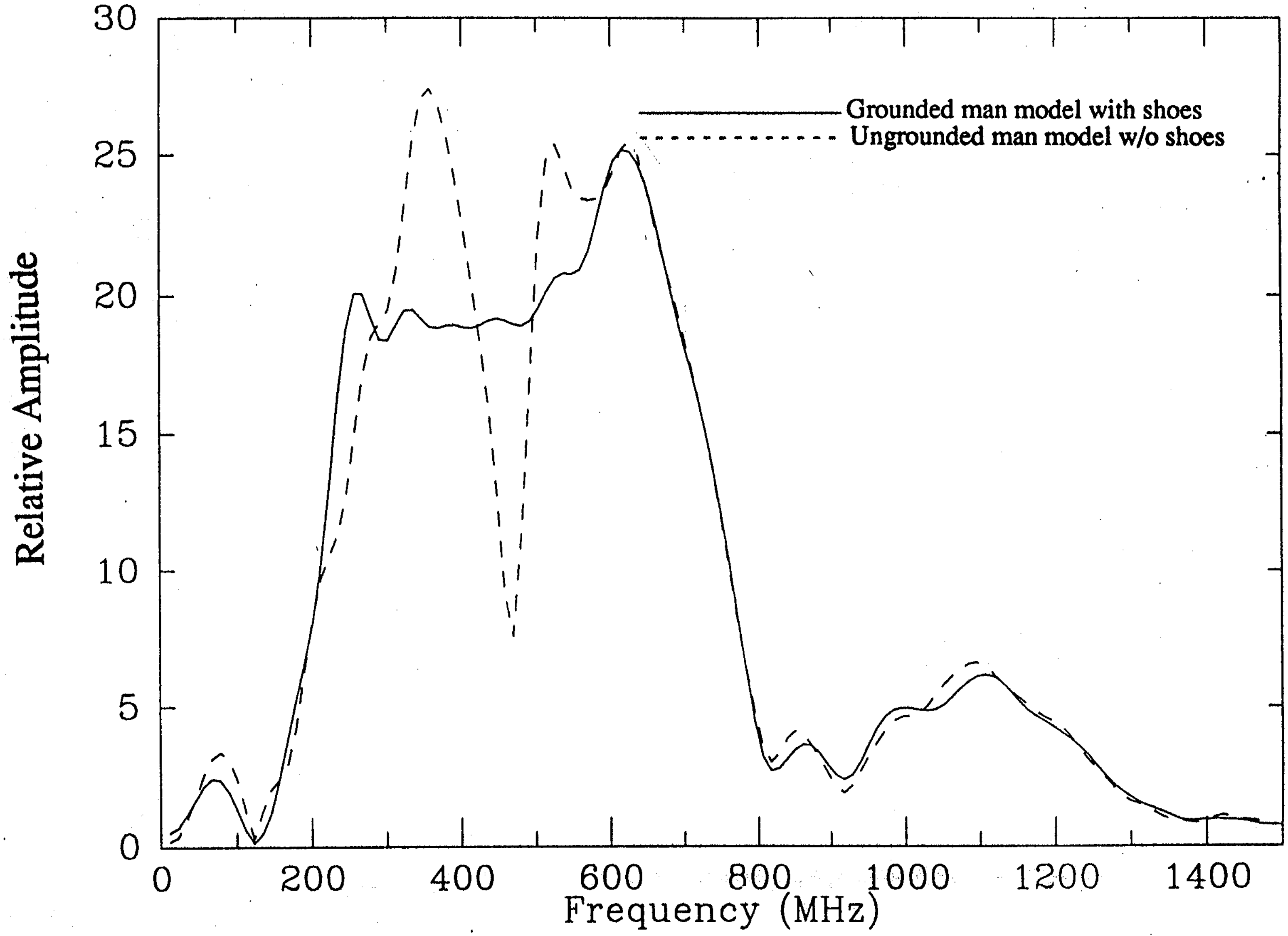

6g. Section through the ankles (height above the bottom of the feet = 13.76 cm).

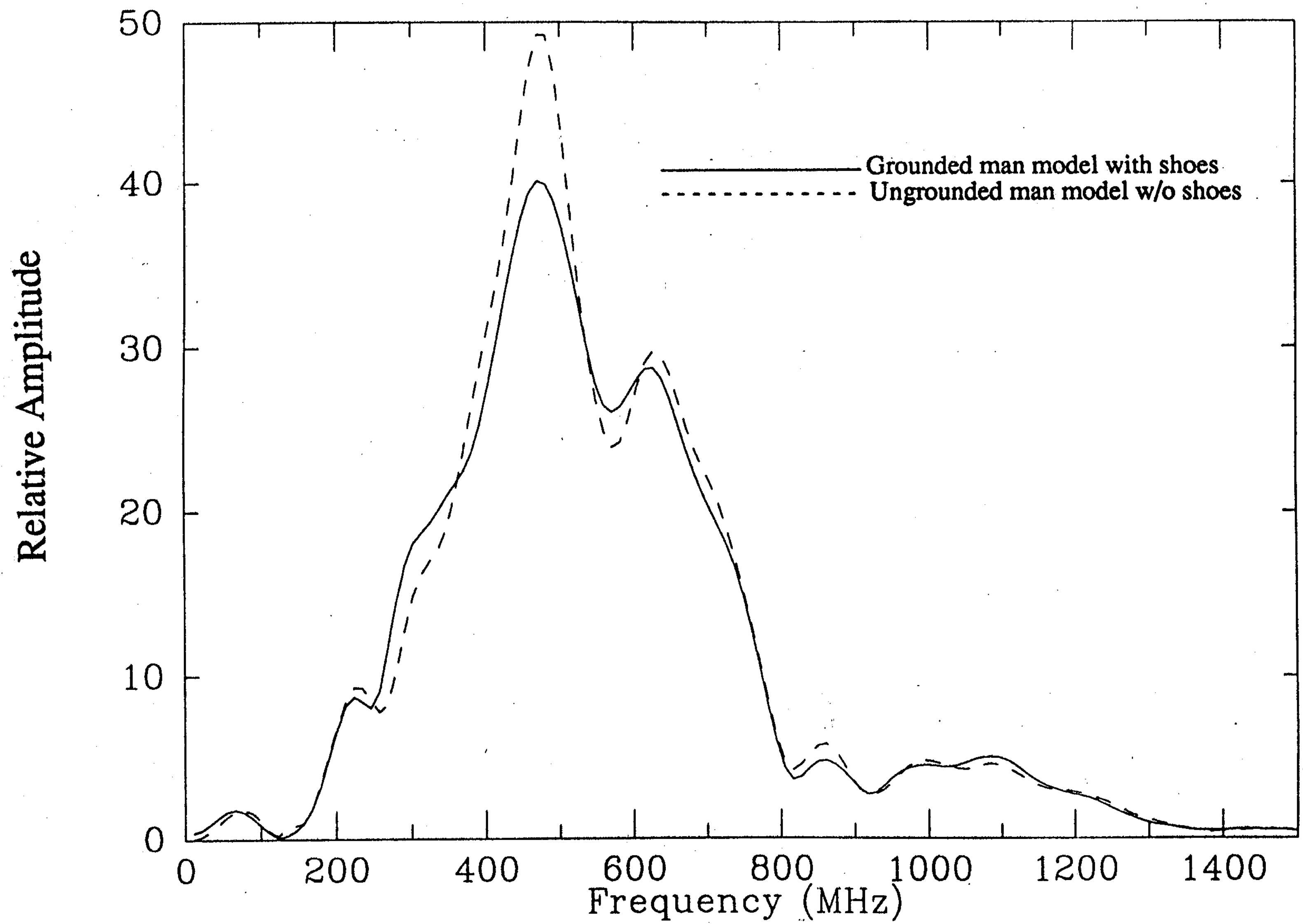

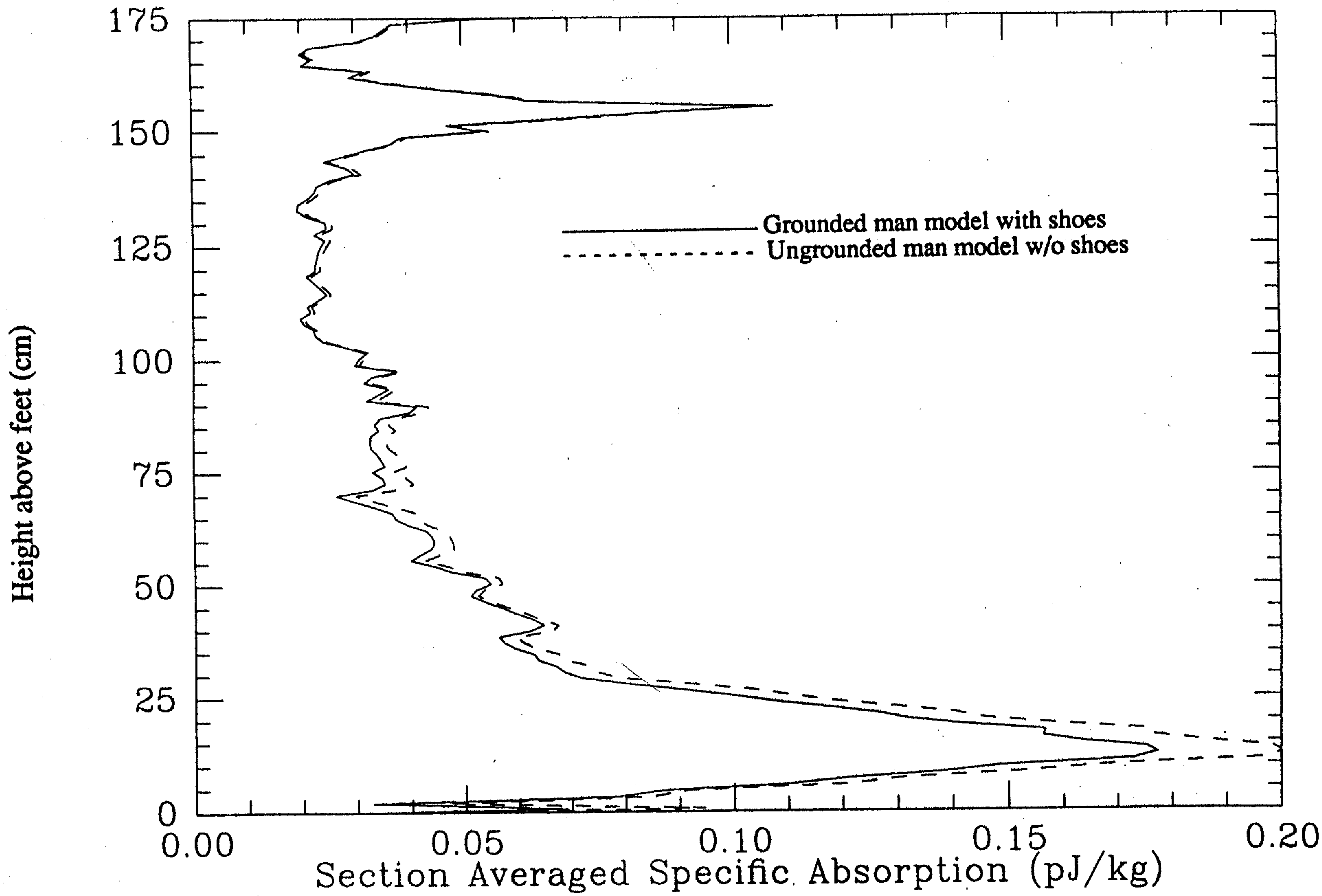

Figure 7. Variation of section or layer-averaged specific absorption for the ultra wideband pulse of Figure 2. E_{peak} = 1.1 V/m.

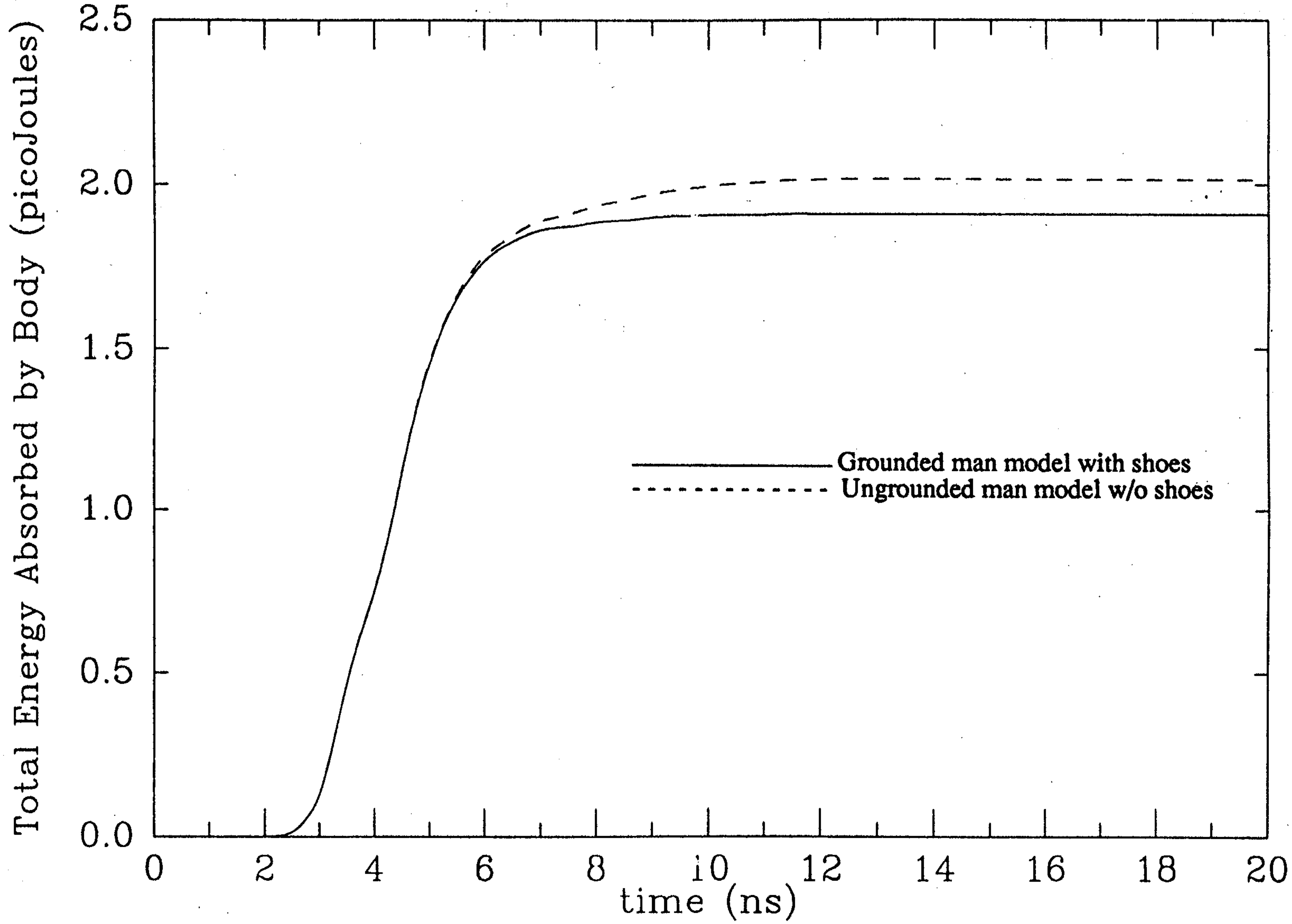

Figure 8. Total energy absorbed by the body as a function of time.